

Secondary electron emission under magnetic constraint: from Monte Carlo simulations to analytical solution

C. Costin^{*}

Iasi Plasma Advanced Research Center (IPARC), Faculty of Physics, Alexandru Ioan Cuza University of Iasi, Iasi-700506, Ro-mania

^{*} claudiu.costin@uaic.ro

April 2, 2024

Abstract

An analytical formula is derived from Monte Carlo simulations for the effective secondary electron emission yield in an oblique magnetic field. It captures the influence of the magnetic field magnitude and tilt, electron emission energy, electron reflection on the surface and electric field intensity on the secondary emission process. The last two parameters increase the effective emission while the others act the opposite. The electric field effect is equivalent to a reduction of the magnetic field tilt. A very good agreement is shown between analytical and numerical solutions for a wide range of parameters. The analytical solution is a convenient tool for theoretical study and design of magnetically assisted applications, providing realistic input for subsequent simulations.

Contents

1	Introduction	1
2	Monte Carlo method	3
3	Analytical solution and results	4
4	Conclusion	8
	References	9

1 Introduction

The International Thermonuclear Experimental Reactor (ITER), the Large Hadron Collider (LHC) and the International Space Station (ISS) are the most ambitious scientific research experiments in their fields, respectively the nuclear fusion research, high-energy particle physics

and space science. Involving huge human and financial resources, worldwide collaborations, they have different goals but they must overcome similar issues. Being part of the larger topic of plasma-surface interaction, one issue is the secondary electron emission (SEE), process consisting in the release of electrons from solid surfaces under the bombardment of primary particles: neutrals, charged particles or photons [1]. Quantitatively, the process is characterized by the SEE yield (SEY), defined as the number of secondary electrons released by a single primary particle. The symbol of the SEY is δ when primary particles are electrons and γ for the others. Regardless of the nature of primary particles, secondary electrons are an important component of the plasma-surface interface, contributing to the charged particles balance at the surface and to the space charge formation. In this respect, various concerns are associated with the SEE process. The secondary electrons cool the plasma and lower the potential drop over the sheath, increasing the heat flux and the electron losses to the surface [2]. For a SEY larger than 1, the space charge may completely vanish [3], leaving the surface fully exposed to plasma. Such effects are of major importance for the optimal operation of fusion devices [4] and space propulsion Hall thrusters [5,6]. Secondary electrons are also responsible for the generation of instabilities in both high-energy accelerators [7,8] and low temperature plasma [9,10]. The performance of high-energy accelerators is limited by the electron cloud effect as result of the secondary emission [8,11]. In space applications, the SEE process leads to electrostatic charging of spacecrafts and satellites, affecting on-board electronic devices [12].

On the other hand, for all electrical discharges governed by Townsend's breakdown theory, the process of SEE induced by ion bombardment at the cathode is essential for both ignition and maintaining the discharge [1,13]. The secondary electrons are used in scanning electron microscopy to form images [14]. Also, the SEY can be used as indicator for the surface cleanliness [15].

Whether it is treated as an issue or not, the control of the SEE process and the accurate knowledge of the SEY are of great importance for both applications and numerical simulations. The SEE is influenced and may be controlled by the presence of a magnetic field at the emitting surface. It is the case of various applications: magnetically confined plasma in fusion devices [16], Hall thrusters [5,6], hollow cathode discharges [17,18] or magnetron sputtering reactors [13,19,20]; electron guidance by magnetic immersion lenses in scanning electron microscopy [21]; magnetic suppression of the SEE from the beam screen of a high-energy accelerator [22] or from the negative electrode of a beam direct energy converter [23].

The magnetic field B guides the secondary electrons on helical trajectories, forcing a certain number of them to return to the emitting surface where they might be reflected or recaptured. If recaptured, the electrons will not generate any relevant effect in the device and they should not be considered further. The direct consequence is a decrease of the SEY down to a value which is often referred to as effective SEY, δ_{eff} or γ_{eff} . The influence of the magnetic field on the effective SEY was investigated both experimentally [16,22–24] and numerically [19,20,25–28]. Detailed analysis is reported in [25] for opened magnetic field lines and in [19] for the particular case of a magnetron discharge. A simple formula was derived for the effective SEY from a fluid model in [20], but with only few parameters and truncated reflection. However, a consistent analytical solution valid for a wide range of parameters, summing up the previous findings and offering an easy-to-use tool is still required.

In this study, a Monte Carlo (MC) simulation method is used to investigate the SEE process in an oblique magnetic field, exploring the effects of electron reflection, electron emission energy and electric field in front of the surface. It is well known that the SEY depends on

the surface (material, temperature and cleanliness condition) and on the primary particle (type, energy and incident angle) [1, 29]. To ensure a generally valid description of the SEE process, the physical quantity calculated and further discussed is the relative SEY $f = \delta_{eff}/\delta$ or $f = \gamma_{eff}/\gamma$. It is independent of the primary particles or surface nature. An analytical formula is derived for the relative SEY f based on the analysis of the numerical results.

2 Monte Carlo method

In the MC simulation, the secondary electrons are randomly released from the surface, obeying a cosine law angular distribution

$$\frac{dN(\theta)}{N_0 d\Omega} = \frac{1}{\pi} \cos \theta, \quad (1)$$

since such distribution is generally accepted regardless of the nature of the primary particle [29, 30]. In (1) $dN(\theta)$ is the number of electrons emitted in the solid angle $d\Omega = \sin \theta d\theta d\varphi$ and N_0 is the total number of secondary electrons.

The energy of the secondary electrons is randomly assigned according to a Maxwell-Boltzmann like distribution:

$$\frac{dN(\epsilon)}{d\epsilon} = C \sqrt{\epsilon} \exp\left(-\frac{\epsilon}{\epsilon_S}\right), \quad (2)$$

with C a normalization constant and ϵ_S the energy (in eV) corresponding to the most probable speed of the secondary electrons. According to [31] the energy distribution function (EDF) of the secondary electrons has basically the same form for all metals, independent of the work function. Unlike other distributions in the literature [32–35], eq. (2) is independent of the surface material and has the advantage of a single fitting parameter. It can also be seen as a simplified form of the EDF derived in [33]. By the right choice of ϵ_S , usually below 10-15 eV, eq. (2) is a good approximation of different distributions reported in the literature [1, 7, 29, 30, 36].

The secondary electrons are moving in a very low background pressure (the collision frequency is much lower than the cyclotron frequency) on collisionless trajectories. Each trajectory is integrated using the leap-frog algorithm coupled with Boris scheme, since it is known to achieve a good balance between accuracy, efficiency and stability for an imposed time step limit $\omega_c \Delta t \leq 0.2$, where $\omega_c = \frac{eB}{m_e}$ is the electron cyclotron frequency [37]. Secondary electrons that return to the surface can be either reflected or recaptured, process described by the reflection coefficient R . If reflected, the electron is returned in the simulation space having the same speed as the incident one, angularly distributed according to (1). Certain electrons may experience multiple reflections.

The time step in the present simulation is 1% of the electron cyclotron period, which corresponds to $\omega_c \Delta t \approx 0.06$. Each electron is tracked either until it is recaptured by the surface or a total integration time of 20 electron cyclotron periods. The latter allows treating a large number of successive reflections, assuring the convergence of eq. (4) to eq. (5) for all investigated conditions. N_0 is 10^4 for all computations.

The magnetic field is homogeneous, tilted by an angle θ_B relative to the surface normal. Magnetic field lines are open, leaving the surface and closing to infinity. An electrostatic sheath is considered in front of the surface, with a constant electric field E pointing perpendicularly towards the surface. The electric field acts along the entire trajectory of the

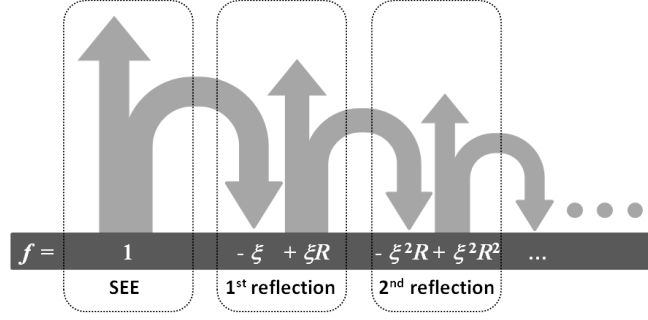


Figure 1: Schematic of the SEE process with multiple reflections.

secondary electrons, assuming that the sheath thickness is larger than the Larmor radius of the secondary electrons. This is a valid assumption for magnetic fields of the order of 0.1–1 T, as in magnetron sputtering devices [19] and tokamaks [25], but it may fail for lower magnetic fields (~ 0.01 T), as in Hall thrusters [6] and hollow cathode discharges [17, 18].

3 Analytical solution and results

The first step in obtaining an accurate analytical expression for the relative SEY f is the analysis of the reflection process, schematically shown in Fig. 1. Without magnetic field, the relative SEY is $f = 1$. With magnetic field, a certain fraction of the secondary electrons ξ returns to the surface. This fraction is more important as the angle of the magnetic field θ_B increases. From the returned fraction ξ , a sub-fraction ξR is reflected back into the simulation space. Thus, after the first reflection, the relative SEY loses the fraction $\xi(1-R)$. The reflected sub-fraction ξR will experience the same cycle. After n successive reflections on the surface, the relative SEY can be written as:

$$f = 1 - \xi(1 - R) - \xi^2 R(1 - R) - \dots - \xi^n R^{n-1}(1 - R), \quad (3)$$

which is a power series having the sum:

$$f = 1 - \xi(1 - R) \frac{1 - (\xi R)^n}{1 - \xi R}. \quad (4)$$

Since both ξ and R are smaller than 1, the term $(\xi R)^n$ tends to zero for an infinite number of reflections ($n \rightarrow \infty$) and the relation (4) converges to:

$$f = \frac{1 - \xi}{1 - \xi R}. \quad (5)$$

Equation (5) is a generally valid formula that defines the relative SEY in the case of multiple reflections of secondary electrons on the emissive surface. It can be customized for particular cases by explicitly including the returning fraction ξ . In the limit case of $R = 1$, the relative SEY is 1 regardless of the value of any other parameter. In the absence of an electrostatic sheath to the surface ($E = 0$ V/m) and without reflection ($R = 0$), MC calculations show (Fig. 2) that the relative SEY is described by:

$$f|_{E=0, R=0} = \cos \theta_B. \quad (6)$$

Equalizing (6) and (5) it comes out that the fraction of secondary electrons that return to the surface due only to the magnetic field is:

$$\xi|_{E=0} = 1 - \cos \theta_B. \quad (7)$$

Introducing (7) in (5) we obtain:

$$f|_{E=0} = \frac{\cos \theta_B}{1 - R(1 - \cos \theta_B)}. \quad (8)$$

Equation (8) is the analytical formula of the relative SEY in an oblique magnetic field, for a surface that emits and reflects electrons with a cosine angular distribution, without electric field to the surface. It also applies when the Larmor radius is much larger than the sheath thickness (low magnetic fields) and the effect of the electric field becomes negligible. Fig. 2 shows a perfect agreement between the analytical expression (8) and the MC calculations for all possible angles and different electron reflection coefficients. In accordance with previous findings, the relative SEY decreases with θ_B [25] and increases with R [19,20]. The inclination of the magnetic field reduces f from 1 ($\theta_B = 0^\circ$) to 0 ($\theta_B = 90^\circ$). Simulations show that, in the absence of an electric field, the relative SEY does not depend on the magnetic flux density B or the EDF of the secondary electrons, hence $f|_{E=0} = f(\theta_B, R)$, in accordance with the results reported in [25].

Even if the EDF of the secondary electrons does not explicitly appear in (8), the reflection coefficient R might depend on the energy of the incident electrons [7,8,11] which, in this case, originate from the secondary electrons. So, there might be an indirect dependence of $f|_{E=0}$ on the EDF of the secondary electrons. This aspect was not analyzed due to the large dispersion of values reported in the literature on the reflection coefficient R . Not only does R depend on the surface material [35–38] and the chemical state of the surface [11,39], but even for the same material (e.g. Cu) the reported results are scattered [7,11,39,40]. Consequently, each case with variable R should be treated separately.

In the presence of an electrostatic sheath to the surface ($E \neq 0$ V/m), MC calculations show that the relative SEY depends on more parameters than in eq. (8), namely $f = f(\theta_B, R, E, B, \epsilon_S)$. The dependence of f on ϵ_S reflects in fact the dependence of f on the EDF of the secondary electrons. The analysis of the emission angular distribution of the recaptured electrons (not shown) indicates that the presence of the electric field is equivalent to a reduction of the magnetic field inclination with respect to the surface normal. The simulation results show that the reduced angle θ_{BE} can be expressed as:

$$\theta_{BE} = \theta_B(1 - A \cos \theta_B), \quad (9)$$

where

$$A = \frac{2E}{Bv_S} \quad (10)$$

and v_S is the most probable speed of the secondary electrons:

$$v_S = \sqrt{\frac{2e\epsilon_S}{m_e}}. \quad (11)$$

The fraction ξ that returns to the surface due to the combined action of E and B is obtained by replacing the angle θ_B with θ_{BE} in (7). Introducing now ξ in (5), the simplified form of f is written as:

$$f = \frac{\cos \theta_{BE}}{1 - R(1 - \cos \theta_{BE})}, \quad (12)$$

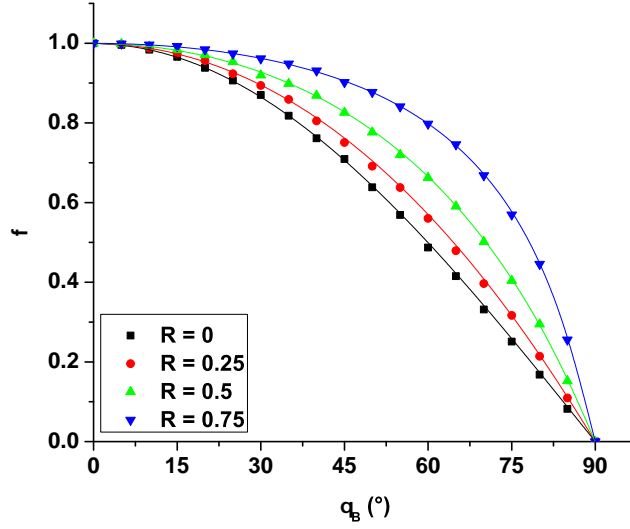


Figure 2: Dependence of the relative SEY on the magnetic field angle θ_B , for different reflection coefficients, in the absence of an electric field. Symbols correspond to MC simulations, full lines correspond to eq. (8).

with θ_{BE} given by (9). Including (9)-(11) in (12), the simple dependence $f = f(\theta_{BE}, R)$ turns into the more general $f = f(\theta_B, R, E, B, \epsilon_S)$. The analytical formula (12) describes the SEE process under the combined action of E and B , for a surface that emits and reflects electrons with a cosine angular distribution. It provides a straightforward solution for the calculation of the relative SEY. Equation (8) is a particular case of (12) for $E = 0$ V/m. Simulation results with different E , B and ϵ_S (not shown) reveal that f depends only on the value of A , regardless of the combination of the three parameters. Therefore, the relative SEY can be expressed as $f = f(\theta_B, R, A)$. The consistency of formula (12) is validated in Fig. 3 by comparison with the results of the MC simulation. The relative SEY is plotted for different values of A , with low (Fig. 3(a)) and high (Fig. 3(b)) reflection coefficient.

A very good agreement is found between the MC calculations and the analytical expression (12). The largest deviation that is observed for certain parameters (e.g. $A = 0.5$, θ_B around 30° in Fig. 3(a)) is below 4%. The relative SEY increases with A while the general dependence on θ_B and R remains as discussed for $E = 0$ V/m. Individual influences of E , B and θ_S on f are reflected in the dependence of f on A . They were also discussed in [25], suggesting that the rapid change of f , which according to Fig. 3 is characteristic to large magnetic field angles, depends on the ratio:

$$\frac{E}{B\sqrt{\epsilon_S}}, \quad (13)$$

which is included in A . The fraction (13) was inappropriately associated to the ratio of the $\mathbf{E} \times \mathbf{B}$ drift speed to the emission speed of the secondary electrons. In fact, the variation of f is more complicated than (13). According to (9), f does not depend only on A but on the product $A \cos \theta_B$. This indicates that the parameter that counts for the increase of f in the presence of an electric field is the electric field component parallel to the magnetic field $E_{\parallel} = E \cos \theta_B$ and not the $\mathbf{E} \times \mathbf{B}$ drift velocity. The drift velocity causes electrons to move along the surface, while E_{\parallel} is responsible for the acceleration of electrons along the magnetic

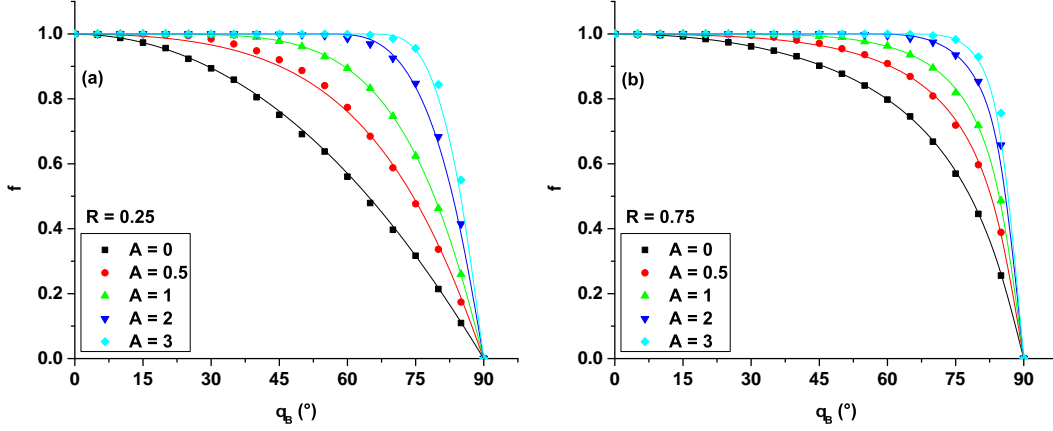


Figure 3: Dependence of the relative SEY on the magnetic field angle θ_B , for two values of the reflection coefficient, (a) $R = 0.25$ and (b) $R = 0.75$, and for different values of the parameter A . Symbols correspond to MC simulations, full lines correspond to eq. (12).

field lines [26]. The two fields E and B act opposite. A higher magnetic flux density enforces smaller gyration radius and shorter cyclotron period for the secondary electrons. The shorter the cyclotron period, the more likely an electron is to return to the surface, which is reflected in a reduction of the relative SEY. A higher electric field, i.e. a higher $E_{||}$, increases the pitch of the helical trajectory, allowing secondary electrons to move away from the surface even in a short cyclotron period. As a result, the relative SEY increases. Higher electron emission energy reduces the relative SEY [28]. A higher velocity component along B , directed to the surface, diminishes the effect of the electric field.

Possible combinations of E and B to obtain a specific value A are shown in Fig. 4, for the energy $\epsilon_S = 5$ eV of the secondary electrons. The influence of ϵ_S is illustrated by plotting the curve $A = 3$ for two more values of ϵ_S (2 and 10 eV). Typical magnetic field values are indicated in Fig. 4 for different applications: 0.01 – 0.03 T for Hall thrusters (HT) and hollow cathode discharges (HC), 0.03 – 0.1 T for magnetron sputtering devices and 1 – 5 T for tokamaks. Customized electric field values can be obtained knowing the electron density and temperature and the surface bias with respect to plasma. For an electric field of 10^5 V/m and $\epsilon_S = 5$ eV, $A > 3$ for HT, $A \approx 3$ for magnetrons and $A \approx 0.1$ for tokamaks.

Equation (9) has physical meaning if θ_{BE} is positive. When θ_{BE} becomes negative, or

$$A \cos \theta_B > 1, \quad (14)$$

none of the secondary electrons return to the surface and the relative SEY is equal to 1. It occurs when the electric field component $E_{||}$ is strong enough to move all secondary electrons away from the surface, regardless of their energy or emission angle. In such a case, the effect of the magnetic field on the SEE is completely suppressed. The inequality (14) is fulfilled for A larger than 1 and $\cos \theta_B > 1/A$. For example, in Fig. 3(a) $f = 1$ for $A = 2$ and $\theta_B < 60^\circ$ or $A = 3$ and $\theta_B < 70.5^\circ$. Figure 4 shows that A larger than 1 is obtained for electric fields larger than $\sim 10^4$ V/m in HT and $\sim 10^6$ V/m in tokamaks.

Including (10)-(11) in (14), an electric field limit E^* can be calculated:

$$E^* = \frac{B}{2 \cos \theta_B} \sqrt{\frac{2e\epsilon_S}{m_e}}, \quad (15)$$

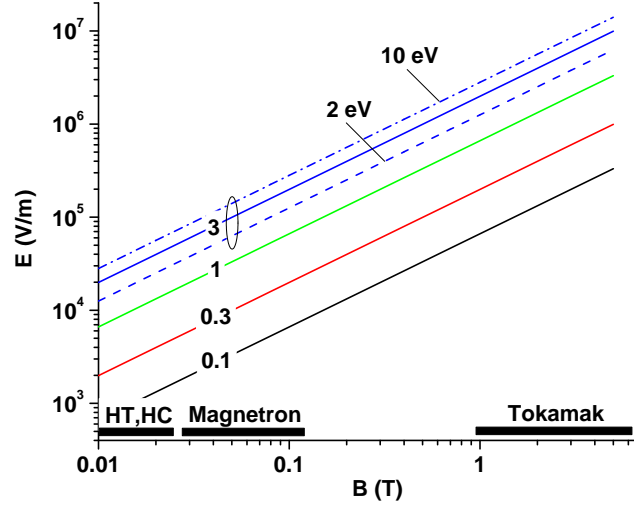


Figure 4: Different electric and magnetic fields combined in (10) to get specific values of the parameter A ($\epsilon_S = 5$ eV except where clearly indicated). Typical magnetic field values for Hall thrusters (HT), hollow cathode discharges (HC), magnetron sputtering devices and tokamaks are indicated.

above which the effect of the magnetic field on the SEE is suppressed. The value of E^* is plotted in Fig. 5 as a function of θ_B angle, for different magnetic flux densities (the same orders of magnitude as for HT, magnetrons and tokamaks) and for $\epsilon_S = 5$ eV. As in Fig. 4, the influence of ϵ_S is illustrated by plotting the curve $B = 0.1$ T for two more values of ϵ_S (2 and 10 eV). At high magnetic field angles $\theta_B > 80^\circ$, the electric field limit E^* increases by an order of magnitude. E^* is not defined when the magnetic field is parallel to the surface ($\theta_B = 90^\circ$), but in this case the relative SEY is zero for all conditions. Reminder: results were obtained assuming non-collisional electron trajectories (very low pressure) and an electrostatic sheath thickness larger than the Larmor radius.

4 Conclusion

The effective secondary electron emission yield in an oblique magnetic field can be calculated with formula (12) which was derived based on the results of Monte Carlo simulations. The magnetic flux density and the emission energy of the secondary electrons contribute to the reduction of the effective SEY. Electron reflection coefficient on the surface acts the opposite. The magnetic field tilt with respect to the surface normal has a major influence on the effective emission. An electric field reduces the magnetic field effect, equivalent to a reduction of the magnetic field tilt. Without electric field, the effective SEY depends only on the magnetic field angle and the reflection coefficient. Formula (12) is a reliable tool for studying the implications of an effective SEE in magnetically assisted devices (tokamaks, magnetrons, Hall thrusters), in scanning electron microscopy, in electron cloud mitigation etc, helping the design of such applications. It also provides realistic input for simulations of already mentioned applications, especially for 0D and 1D codes that are not able to describe the effective SEE process. Further investigations should target the influence of the background

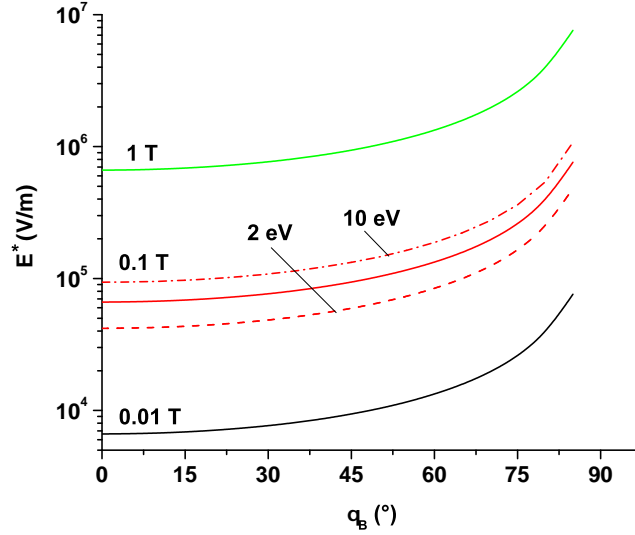


Figure 5: Electric field limit E^* calculated from (15) as a function of the magnetic field angle θ_B , for different magnetic flux densities ($\epsilon_S = 5$ eV except where clearly indicated).

pressure or other angular distributions of the secondary electrons on the effective SEY. A variable electric field along the electrostatic sheath or a spatially limited sheath may also be considered.

References

- [1] B. Chapman, *Glow Discharge Processes: Sputtering and Plasma Etching*, John Wiley and Sons, NY (1980).
- [2] G. D. Hobbs and J. A. Wesson, *Heat flow through a langmuir sheath in the presence of electron emission*, Plasma Phys. **9**, 85 (1967), doi:10.1088/0032-1028/9/1/410.
- [3] M. D. Campanell, A. V. Khrabrov and I. D. Kaganovich, *Absence of debye sheaths due to secondary electron emission*, Phys. Rev. Lett. **108**, 255001 (2012), doi:10.1103/PhysRevLett.108.255001.
- [4] P. J. Harbour and M. F. A. Harrison, *The influence of electron emission at the divertor target of a tokamak fusion reactor*, Journal of Nuclear Materials **76-77**, 513 (1978), doi:10.1016/0022-3115(78)90197-6.
- [5] A. I. Morozov and V. V. Savelyev, *Fundamentals of stationary plasma thruster theory*, In B. B. Kadomtsev and V. D. Shafranov, eds., *Reviews of Plasma Physics*, vol. 21. Springer, Boston, doi:10.1007/978-1-4615-4309-1_2 (2000).
- [6] Y. Raitses, I. D. Kaganovich, A. Khrabrov, N. J. F. D. Sydorenko and A. Smolyakov, *Effect of secondary electron emission on electron cross-field current in exb discharges*, IEEE Transactions on Plasma Science **39**, 995 (2011), doi:10.1109/TPS.2011.2109403.

- [7] M. Izawa, Y. Sato and T. Toyomasu, *The vertical instability in a positron bunched beam*, Phys. Rev. Lett. **74**, 5044 (1995), doi:10.1103/PhysRevLett.74.5044.
- [8] F. Zimmermann, *Review of single bunch instabilities driven by an electron cloud*, Phys. Rev. ST Accel. Beams **7**, 124801 (2004), doi:10.1103/PhysRevSTAB.7.124801.
- [9] M. B. Hendricks, P. C. Smith, D. N. Ruzic, A. Leybovich and J. E. Poole, *Effects of ion-induced electron emission on magnetron plasma instabilities*, J. Vac. Sci. Technol. A **12**, 1408 (1994), doi:10.1116/1.579329.
- [10] M. C. Griskey and R. L. Stenzel, *Secondary-electron-emission instability in a plasma*, Phys. Rev. Lett. **82**, 556 (1999), doi:10.1103/PhysRevLett.82.556.
- [11] R. Cimino, I. R. Collins, M. A. Furman, M. Pivi, F. Ruggiero, G. Rumolo and F. Zimmermann, *Can low-energy electrons affect high-energy physics accelerators?*, Phys. Rev. Lett. **93**, 014801 (2004), doi:10.1103/PhysRevLett.93.014801.
- [12] S. T. Lai, *Fundamentals of Spacecraft Charging: Spacecraft Interactions with Space Plasmas*, Princeton, NY, doi:10.2307/j.ctvc4m4j2n (2002).
- [13] O. Baranov, M. Romanov, S. Kumar, X. X. Zhong and K. Ostrikov, *Magnetic control of breakdown: Toward energy-efficient hollow-cathode magnetron discharges*, Journal of Applied Physics **109**, 063304 (2011), doi:10.1063/1.3553853.
- [14] H. Seiler, *Secondary electron emission in the scanning electron microscope*, J. Appl. Phys. **54**, R1 (1983), doi:10.1063/1.332840.
- [15] L. A. Gonzalez, M. Angelucci, R. Larciprete and R. Cimino, *The secondary electron yield of noble metal surfaces*, AIP Advances **7**, 115203 (2017), doi:10.1063/1.5000118.
- [16] S. Takamura, S. Mizoshita and N. Ohno, *Suppression of secondary electron emission from the material surfaces with grazing incident magnetic field in the plasma*, Physics of Plasmas **3**, 4310 (1996), doi:10.1063/1.871962.
- [17] V. Tiron, I.-L. Velicu, A. V. Nastuta, C. Costin, G. Popa, Z. Kechidi, C. Ionita and R. Schrittwieser, *Enhanced extraction efficiency of the sputtered material from a magnetically assisted high power impulse hollow cathode*, Plasma Sources Sci. Technol. **27**, 085005 (2018), doi:10.1088/1361-6595/aad3ff.
- [18] M. P. Bhuva, S. K. Karkari and S. Kumar, *Influence of cold hollow cathode geometry on the radial characteristics of downstream magnetized plasma column*, Plasma Sources Sci. Technol. **28**, 115013 (2019), doi:10.1088/1361-6595/ab53dc.
- [19] G. Buyle, D. Depla, K. Eufinger and R. D. Gryse, *Calculation of the effective gas interaction probabilities of the secondary electrons in a dc magnetron discharge*, J. Phys. D: Appl. Phys. **37**, 1639 (2004), doi:10.1088/0022-3727/37/12/008.
- [20] C. Costin, G. Popa and G. Gousset, *On the secondary electron emission in dc magnetron discharge*, J. Optoelectron. Adv. Mat. **7**, 2465 (2005).
- [21] M. Toth, W. R. Knowles and B. L. Thiel, *Secondary electron imaging of non-conductors with nanometer resolution*, Applied Physics Letters **88**, 023105 (2006), doi:10.1063/1.2161571.

- [22] V. V. Anashin, I. R. Collins, R. V. Dostovalov, N. V. Fedorov, O. Gröbner, A. A. Krasnov, O. B. Malyshev and E. E. Pyata, *Magnetic and electric field effects on the photoelectron emission from prototype lhc beam screen material*, Vacuum **60**, 225 (2001), doi:10.1016/S0042-207X(00)00392-4.
- [23] K. Hashimoto and T. Sugawara, *Magnetic suppression of secondary electron emission from the negative electrode in a beam direct energy converter*, Fusion Technology **17**, 566 (1990), doi:10.13182/FST90-A29192.
- [24] I. H. Tan, M. Ueda, R. S. Dallaqua, R. de Moraes Oliveira and J. O. Rossi, *Magnetic field effects on secondary electron emission during ion implantation in a nitrogen plasma*, J. Appl. Phys. **100**, 033303 (2006), doi:10.1063/1.2201695.
- [25] S. Mizoshita, K. Shiraishi, N. Ohno and S. Takamura, *Secondary electron emission from solid surface in an oblique magnetic field*, Journal of Nuclear Materials **220-222**, 488 (1995), doi:10.1016/0022-3115(94)00509-5.
- [26] K. Nishimura, K. Ohya and J. Kawata, *Secondary electron, emission from beryllium irradiated by plasmas in a magnetic field*, Vacuum **47**, 959 (1996), doi:10.1016/0042-207X(96)00102-9.
- [27] Y. Igitkhanov and G. Janeschitz, *Attenuation of secondary electron emission from divertor plates due to magnetic field inclination*, J. Nucl. Mat. **290-293**, 99 (2001), doi:10.1016/S0022-3115(00)00560-2.
- [28] D. Tskhakayaa and S. Kuhn, *Influence of initial energy on the effective secondary-electron emission coefficient in the presence of an oblique magnetic field*, Contrib. Plasma Phys. **40**, 484 (2000), doi:10.1002/1521-3986(200006)40:3/4<484::AID-CTPP484>3.0.CO;2-E.
- [29] H. Bruining, *Physics and Applications of Secondary Electron Emission*, Pergamon Press, London (1954).
- [30] R. Kawakami, J. Kawata and K. Ohya, *Simultaneous calculation of reflection, physical sputter-ing and secondary electron emission from a metal surface due to impact of low-energy ions*, Jpn. J. Appl. Phys. **38**, 6058 (1999), doi:10.1143/JJAP.38.6058.
- [31] E. J. Sternglass, *Theory of secondary electron emission by high-speed ions*, Physical Review **108**, 1 (1957), doi:10.1103/PhysRev.108.1.
- [32] M. S. Chung and T. E. Everhart, *Simple calculation of energy distribution of low energy secondary electrons emitted from metals under electron bombardment*, J. Appl. Phys. **45**, 707 (1974), doi:10.1063/1.1663306.
- [33] C. Bouchard and J. D. Carette, *The surface potential barrier in secondary emission from semiconductors*, Surf. Sci. **100**, 251 (1980), doi:10.1016/0039-6028(80)90456-2.
- [34] J. J. Scholtz, D. Dijkkamp and R. W. A. Schmitz, *Secondary electron emission properties*, Philips Journal of Research **50**, 375 (1996), doi:10.1016/S0165-5817(97)84681-5.
- [35] J. Cazaux, *Reflectivity of very low energy electrons (< 10 eV) from solid surfaces: Physical and instrumental aspects*, J. Appl. Phys. **111**, 064903 (2012), doi:10.1063/1.3691956.

- [36] M. I. Patino, Y. Raitses, B. E. Koel and R. E. Wirz, *Analysis of secondary electron emission for conducting materials using 4-grid leed/aes optics*, J. Phys. D: Appl. Phys. **48**, 195204 (2015), doi:10.1088/0022-3727/48/19/195204.
- [37] C. K. Birdsall and A. B. Langdon, *Plasma Physics via Computer Simulations*, IOP Publishing, NY, doi:10.1201/9781315275048 (1991).
- [38] V. I. Demidov, S. F. Adams, I. D. Kaganovich, M. E. Koepke and I. P. Kurlyandskaya, *Measurements of low-energy electron reflection at a plasma boundary*, Phys. Plasmas **22**, 104501 (2015), doi:10.1063/1.4933002.
- [39] E. G. McRae and C. W. Caldwell, *Very low energy electron reflection at cu(001) surfaces*, Surface Science **57**, 77 (1976), doi:10.1016/0039-6028(76)90169-2.
- [40] I. Gimpel and O. Richardson, *The secondary electron emission from metals in the low primary energy region*, Proc. R. Soc. Lond. A **182**, 17 (1943), doi:10.1098/rspa.1943.0022.